



Research paper

Long-term efficacy and safety of mRNA therapy in two murine models of methylmalonic acidemia

Ding An, Andrea Frassetto, Eric Jacquinet, Marianne Eybye, Joseph Milano, Christine DeAntonis, Vi Nguyen, Rodrigo Laureano, Jaclyn Milton, Staci Sabnis, Christine M. Lukacs, Lin T. Guey*

Moderna, Inc., 200 Technology Square, Cambridge, MA 02139, USA

ARTICLE INFO

Article history:

Received 17 May 2019

Received in revised form 24 June 2019

Accepted 1 July 2019

Available online 12 July 2019

Keywords:

Enzyme replacement

Liver targeted therapy

Methylmalonyl-CoA mutase

Organic acidemia

Systemic mRNA therapy

ABSTRACT

Background: Isolated methylmalonic acidemia/aciduria (MMA) is an ultra-rare, serious, inherited metabolic disorder with significant morbidity and mortality. Exogenously delivered mRNA encoding human methylmalonyl-CoA mutase (hMUT), the enzyme most frequently mutated in MMA, is a potential therapy to produce functional MUT enzyme in liver.

Methods: Two 12-week repeat-dose studies were conducted to evaluate the efficacy and safety of intravenously-administered hMUT mRNA encapsulated in lipid nanoparticles in two murine models of MMA.

Findings: In MMA hypomorphic mice, hMUT mRNA treatment resulted in dose-dependent and reproducible biomarker responses after each dose. Enzymatically-active MUT protein was produced in liver in a dose-dependent manner. hMUT mRNA was well-tolerated with no adverse effects, as indicated by the lack of clinical observations, minimal changes in clinical chemistry parameters, and histopathology examination across all tissues. In severe MMA mice, hMUT mRNA led to substantially improved survival and growth and ameliorated biochemical abnormalities, all of which are cardinal clinical manifestations in severely affected patients.

Interpretation: These data demonstrate durable functional benefit of hMUT mRNA and support development of this new class of therapy for a devastating, pediatric disorder.

Fund: This work was funded by Moderna, Inc.

This is an open access article under the CC BY-NC-ND license (<http://creativecommons.org/licenses/by-nc-nd/4.0/>).

1. Introduction

Isolated methylmalonic acidemia/aciduria (MMA) is an ultra-rare, devastating, life-threatening inherited metabolic disorder with no approved therapies that address the underlying defect. It is primarily caused by a defect or deficiency in the vitamin B₁₂-dependent mitochondrial enzyme, methylmalonyl-coenzyme A (CoA) mutase (MUT, EC 5.4.99.2) [1,2]. The deficiency in MUT causes a metabolic block in the propionate metabolism pathway, resulting in marked accumulation of toxic metabolites such as methylmalonic acid (the name-giving organic acid) [1,3–5]. MMA due to MUT deficiency (OMIM #251000) can be further classified into defects without (mut⁰) or with residual (mut⁻) enzyme activity.

MMA is a pediatric disorder with significant morbidity and mortality. Despite dietary and supportive management, the overall long-term outcomes for MMA patients remain poor, particularly for mut⁰ patients [4–6]. Patients suffer from numerous complications, including

growth retardation, chronic renal failure, neurologic complications, and intermittent life-threatening metabolic decompensations [4–6]. Elective liver transplantation (LT), or combined liver-kidney transplantation (LKT) for patients with renal failure, have emerged as potential treatment options for severely affected individuals. Transplanted patients display substantial reductions in circulating methylmalonic acid and markedly fewer metabolic decompensations [7–12]. While the transplant experience highlights liver as a major metabolic organ for the disorder, LT/LKT as a treatment option is limited by the risks of the procedure itself and the availability of donors. Thus, there remains a dire unmet medical need in this population.

Exogenously delivered mRNA therapy is emerging as a new therapeutic modality with the potential to treat myriad disorders including mitochondrial enzymopathies like MMA. Systemic administration of mRNA encapsulated in lipid nanoparticle (LNP) primarily induces protein expression in liver [13–17]. Low levels of expression of protein have also been reported in spleen [17]. Within the liver, hepatocytes are the primary target cell type, where dose-dependent protein expression has been observed following systemic administration of a reporter mRNA encoding enhanced green fluorescent protein (eGFP)

* Corresponding author.

E-mail address: Lin.Guey@Moderna.com (L.T. Guey).

Research in context

Evidence before this study

Isolated MMA is a pediatric disorder with significant morbidity and mortality. The disorder is primarily caused by a defect or deficiency in the mitochondrial enzyme, MUT. There are no approved therapies that address the underlying defect of the disorder. Despite dietary and supportive management, the overall long-term outcomes for MMA patients remain poor. Thus, there remains a dire unmet medical need in this population. Previous preclinical in vitro and short-term in vivo studies demonstrated proof-of-concept for *hMUT* mRNA as a novel therapeutic approach to restore functional enzyme in liver.

Added value of this study

We describe a comprehensive preclinical evaluation of the long-term efficacy, safety and tolerability of *hMUT* mRNA therapy in two separate 12-week studies in two different murine models of MMA that represent the spectrum of MUT deficiency. These studies demonstrate sustained pharmacology and durable functional benefit for *hMUT* mRNA in relevant murine models of disease. Additionally, *hMUT* mRNA therapy was well-tolerated with no adverse side effects in both mouse models.

Implications of all the available evidence

These data collectively support the clinical development of this investigational mRNA medicine for a devastating, pediatric, inherited metabolic disorder with no other effective treatment options other than solid organ transplantation.

encapsulated in LNPs [17]. LNP-encapsulated mRNA is internalized by hepatocytes via opsonization of LNPs by apolipoprotein E (ApoE) followed by receptor-mediated endocytosis [18].

Full realization of the potential of systemic mRNA therapy requires the ability to achieve long-term efficacy and safety upon repeated systemic dosing of mRNA, due to the limited duration of mRNA-encoded proteins. Although preclinical proof-of-concept studies have evaluated mRNA-encoded intracellular and secreted therapeutic proteins in various animal models of disease with liver as the target organ [17,19–25], the ability to chronically, effectively and safely dose exogenous mRNAs with consistent and sustained pharmacology in long-term preclinical studies has not been reported to date. Furthermore, additional long-term studies evaluating *hMUT* mRNA are required to support the clinical development of this novel therapy in a primarily pediatric population. Here, we describe a comprehensive preclinical evaluation of the long-term efficacy, safety and tolerability of *hMUT* mRNA therapy in two separate 12-week studies in two murine models of MMA that represent the spectrum of MUT deficiency. These studies underscore the durable functional benefit of mRNA therapy to potentially treat this devastating pediatric disorder.

2. Materials and methods

2.1. mRNA production and formulation

mRNA was synthesized and formulated in LNPs as described previously [26–28]. The same biodegradable, ionizable LNP described in our previous studies [19] was used in the current set of studies. The full sequences of *hMUT* mRNA and *eGFP* mRNA are specified in Table S1 and Table S2 respectively. Briefly, mRNA was synthesized in vitro by

T7 RNA polymerase-mediated transcription with 5-methoxy UTP in place of UTP. The linearized DNA template incorporates the 5' and 3' untranslated regions (UTRs) and the poly-A tail. After purification, the mRNA was diluted in 50 mM sodium acetate (pH 5) and mixed with lipids dissolved in ethanol (50:10:38.5:1.5; ionizable: helper: structural: polyethyleneglycol) at a ratio of 3:1 (mRNA:lipids). The final product was filtered through a 0.22 μ m filter and stored in pre-sterilized vials frozen until use. All formulations were tested for particle size, RNA encapsulation, and endotoxin and were found to be <100 nm in size, with >80% encapsulation, and <10 EU/mL endotoxin.

2.2. Murine models of methylmalonic acidemia

Animals studies were approved by the Institutional Animal Care and Use Committee at Moderna. *Mut*^{-/-} mice harbor a deletion of exon 3 which encodes the putative substrate-binding pocket in the MUT enzyme. This *Mut* allele is null and unable to produce mature RNA or protein [29,30]. *Mut*^{-/-};Tg^{INS-MCK-Mut} mice express the *Mut* gene under the control of a muscle-specific creatine kinase (*MCK*) promoter which results in the rescue of mice from neonatal lethality; however, these mice display significant mortality, severe metabolic perturbations, growth retardation, and a hepatorenal mitochondriopathy [31]. Levels of plasma methylmalonic acid, a key toxin that accumulates directly due to the causative enzymatic deficiency, are massively elevated compared to wild type littermates and are similar to levels found in severe MMA patients [31]. *Mut*^{-/-};Tg^{INS-CBA-G715V} hypomorphic mice ubiquitously express a mouse orthologue (p.G715 V) of a mutation described in MMA *mut*⁻ patients (p.G717 V) under the control of an enhanced chicken β -actin (*CBA*) promoter in *Mut*^{-/-} mice [32]. Similar to *mut*⁻ patients, these mice have reduced but not complete loss of MUT enzyme activity resulting in significant elevations of disease-associated toxic metabolites such as methylmalonic acid. These mice have decreased MUT activity in all tissues and moderately increased plasma methylmalonic acid concentrations in the blood, similar to MMA patients harboring the p.G717 V mutation [32]. *Mut*^{+/-} mice were used as littermate controls in the current study given that their biochemical parameters are identical to *Mut*^{+/+} mice [33].

Sample sizes for the 12-week repeat dose studies in both murine models of MMA were determined from power calculations. For the 12-week study in MMA hypomorphic (*Mut*^{-/-};Tg^{INS-CBA-G715V}) mice, a sample size of $n = 11$ /group was determined based on power calculations to detect a > 50% decrease in plasma methylmalonic acid concentrations between treated and control arms with 80% power and 5% significance level assuming a two-tailed unpaired *t*-test and equal variances between groups. For the 12-week study in the more severe MMA murine model (*Mut*^{-/-};Tg^{INS-MCK-Mut}), a sample size of $n = 6$ /group was determined from power calculations using a two-tailed log-rank test to detect a $\geq 70\%$ difference of survival rates between treatment arms assuming 15% and 85% survival rates in control and treatment arms, respectively, with 80% power and 5% significance level. All study groups were equally balanced for male and female mice. Groups in the MMA hypomorphic mouse study consisted of 4–8 week old $n = 5$ –6 female and $n = 5$ –6 male mice. Similarly, groups in the 12-week study in severe MMA *Mut*^{-/-};Tg^{INS-MCK-Mut} mice consisted of 3–6 week old $n = 3$ female and $n = 3$ male mice. A group of unaffected *Mut*^{+/-} littermate control mice were included in both studies ($n = 11$ [6 female, 5 male] in the hypomorphic study, $n = 6$ [3 female, 3 male] in the severe MMA mouse study). A separate cohort ($n = 5$; 2 female, 3 male) of 6–11 week old *Mut*^{-/-};Tg^{INS-MCK-Mut} mice was utilized to evaluate endogenous tissue biomarker concentrations for the 12-week study in severe MMA mice.

All mice were randomly assigned to study groups based on age and body weight. IV injections were administered via the tail vein. In-life blood collection was via submandibular bleed and terminal blood collection was by cardiac puncture. Mice were perfused prior to tissue collection to avoid blood contamination.

2.3. Clinical observations

Clinical observations were performed and recorded at least 5 times per week in both studies. Detailed clinical observations included, but were not limited to, identification of clinical signs related to: general appearance (e.g., skin, fur, changes in eyes, eyeballs and mucous membranes; presence or absence of discharge), body position and posture (e.g., hunchback posture), autonomic nervous system function (e.g., lacrimation, piloerection, pupil diameter, respiration, excretion), motor coordination, ambulatory abnormalities, reaction to being handled and to environmental stimulation, nervous system (e.g., tremor, convulsion, muscular contractions), changes in exploratory behavior, ordinary behavior (e.g., changes in grooming, headshaking, gyration), abnormal behavior (e.g., autophagia, backward motion, abnormal vocalization) and aggression.

2.4. Quantification of plasma methylmalonic acid, 2-methylcitrate, C3 and C2 concentrations

Plasma methylmalonic acid and 2-methylcitrate were analyzed and quantified by liquid chromatography–tandem mass spectrometry (LC-MS/MS) as described previously [34]. C3 and C2 carnitine concentrations were quantified by ion-exchange solid-phase extraction, derivatized with pentafluorophenacyl trifluoromethanesulfonate, separated by high performance liquid chromatography, and detected with an ion trap mass spectrometer as described previously [35]. The lower levels of quantification (LLOQ) for these metabolite assays are: 5 or 10 μM , depending on the dilution, for plasma methylmalonic acid, 0.5 μM for 2-methylcitrate, 0.1 μM for plasma C3, and 2 μM for plasma C2. Values below the LLOQ were imputed as 0.

2.5. Quantification of tissue methylmalonic acid and 2-methylcitrate levels

Tissue samples were homogenized using an Omni Bead Ruptor following addition of 4 eq (w/v) of 80:20 water: acetonitrile. Methylmalonic acid and 2-methylcitrate extracts were derivatized with BuOH/HCl to generate the corresponding butyl ester derivatives of each analyte respectively and analyzed and quantified by LC-MS/MS as described previously [34]. The LLOQs are: 0.1 $\mu\text{mol/g}$ tissue or 0.2 $\mu\text{mol/g}$ tissue, depending on the dilution, for tissue methylmalonic acid and 10 nmol/g tissue for 2-methylcitrate. Values below the LLOQ were imputed as 0. All metabolite assays for plasma and tissue matrices were conducted in a blinded fashion.

2.6. Quantification of tissue hMUT protein levels

hMUT protein concentrations in mouse tissues following hMUT mRNA administration were quantified by LC-MS/MS in a blinded fashion. Tissues were homogenized in 100 mM ammonium bicarbonate buffer with 8 M urea. Human MUT isotopically labeled signature peptides (human MUT specific peptide, IIADIFEYTA^{*}, in which natural carbon and nitrogen atoms on lysine were fully replaced with ¹³C and ¹⁵N isotopes, respectively; Thermo Pierce, Rockford, IL) were used as internal standards and spiked into each sample. Liver proteins were denatured, followed by reduction using 5 mM tris (2-carboxyethyl) phosphine hydrochloride (75,259, Sigma-Aldrich Inc., St. Louis, MO) at 37 °C for 1 h, alkylation with 10 mM iodoacetamide (16125, Sigma-Aldrich Inc., St. Louis, MO) at 25 °C in the dark, and then digestion at 37 °C for 15 h with trypsin (trypsin:protein = 1:50 w/w; Catalog #V5280, Promega Inc., Madison, WI). The trypsin digestion reaction was stopped by adding formic acid (28,905, Thermo Fisher Scientific, Waltham, MA). Samples were desalted on the SOLA plate (60309–001, Thermo Fisher Scientific, Waltham, MA), dried, and resuspended in water with 2% acetonitrile and 0.1% formic acid (A955–1, LS120–1, Fisher Scientific, Waltham, MA). Total protein (0.25 μg) was loaded onto the column (75 $\mu\text{m} \times 15$ cm column packed with Waters Acquity

BEH resin 1.7 $\mu\text{m} \times 130$ Å) and subjected to LC-MS/MS analysis (Thermo Easy 1000 nano-UPLC, Orbitrap Fusion Mass Spectrometer, Thermo Fisher Scientific, Waltham, MA). Water (A) and acetonitrile (B) with 0.1% formic acid were used for LC separation. The flow rate was 300 nL/min. The gradient was as follows: 2% B to 7% B in 5 min; 7% to 35% B in 45 min; 35% to 80% B in 5 min; 80% to 95%B in 2 min; and 95% B for 5 min. The mass spectrometry was performed in continuous PRM mode: spray voltage: 1900 V; S-lens RF: 60%; isolation width: 1.4 m/z; HCD: 30% collision energy; detector: orbitrap; resolution: 60,000; scan range: 100–1800 m/z; AGC: 5E4; max injection time: 200 ms. The LLOQ was 0.5 ng/mg protein and values below the LLOQ were imputed as 0.

2.7. Quantification of total MUT enzyme activity in liver

MUT activity was determined by methods described previously [36]. Briefly, lysates were incubated with 5'-deoxyadenosylcobalamin (200 μM , C0884, Sigma-Aldrich Inc., St. Louis, MO) and a racemic mix of methylmalonyl-CoA (1 mM; M1762, Sigma-Aldrich Inc., St. Louis, MO) at 37 °C for 15 min. MUT enzyme reactions were terminated by the addition of 100 g/L trichloroacetic acid (2.5%; T6399 Sigma-Aldrich Inc., St. Louis, MO) with vortexing. Samples were centrifuged at 13,000g for 5 min. Chromatographic separation and quantification were accomplished with HPLC. Supernatants (20 μL) were injected and separated on a Poroshell EC-C18 120 HPLC column (695975–302, Agilent Technologies, Santa Clara, CA) equilibrated with 100 mM acetic acid (A6283, Sigma Aldrich Inc., St. Louis, MO) in 100 mM sodium phosphate (AC343815000, Fisher Scientific, Waltham, MA) buffer, pH 7.0 (Solvent A). Solvent B was prepared by addition of 18% v/v methanol in Solvent A. Elution was performed with a linear methanol gradient: Solvent B increased from 0 to 95% from 0 to 15 min (95% Solvent B) and then stayed at 95% from 15 to 25 min (95%) with a flow rate of 0.5 mL/min.

2.8. Clinical chemistry panel

Blood samples were collected into a syringe and then transferred into serum separator tubes and allowed to clot for at least 20 min (not to exceed 1 h), then centrifuged at room temperature for at least 15 min. The resulting serum samples were frozen on dry ice as soon as possible until stored in a freezer set to maintain -20 °C until shipment to IDEXX (3 Centennial Dr., North Grafton, MA 01536) for sample analysis. Clinical chemistry parameters were measured in a blinded manner by a standard chemistry analyzer as described by IDEXX.

2.9. Histopathology

Histopathological evaluation was performed by an experienced veterinary pathologist on a full panel of tissues identified in Table S5 from all mice at the end of the 12-week study in MMA hypomorphic mice. Tissues were collected and embedded in paraffin, sectioned, mounted on glass slides, and stained with hematoxylin and eosin. A complete gross pathological examination was performed in addition to a detailed microscopic evaluation of all tissues.

2.10. Statistical analysis

All data are presented as mean \pm standard error of the mean (SEM). Statistical analyses and descriptive statistics were performed using Prism 7 (GraphPad) or SAS version 9.4. The D'Agostino and Pearson normality test was performed to ensure the data met the normality assumptions of statistical tests. A repeated measures ANOVA was performed to analyze plasma disease biomarkers from the 12-week study in MMA hypomorphic mice. Continuous variables assessed at the end of the study (e.g. tissue biomarkers concentrations, liver hMUT protein and enzyme activity, clinical chemistry) were analyzed with a one-way ANOVA followed by Dunnett's or Tukey's post-hoc

pairwise comparisons tests or its nonparametric equivalent. Categorical variables were analyzed using Fisher's exact test. The log-rank test was used to compare survival curves between study groups in the 12-week study in severe MMA mice. Plasma disease biomarkers in severe MMA mice were compared to pre-treatment baseline levels using paired *t*-tests. Two-tailed *p* values <.05 were considered statistically significant.

3. Results

3.1. Dose-dependent amelioration of biochemical abnormalities in a 12-week study in MMA hypomorphic mice

A 12-week repeat dose study was conducted in a hypomorphic murine model of MMA MUT deficiency (*Mut*^{-/-};Tg^{INS-CBA-G715V}) to evaluate the long-term efficacy, safety and tolerability of *hMUT* mRNA formulated in LNPs. Baseline (pre-treatment) characteristics of age, sex, body weight (Table S3) and plasma biomarkers (Fig. 1a–c) were similar across all study groups in MMA hypomorphic mice.

To determine the optimal dosing interval, plasma biomarkers were monitored for 4 weeks following a single IV injection of PBS control, *eGFP* control mRNA formulated in LNPs (2 mg/kg), or *hMUT* mRNA formulated in LNPs (0.1, 0.5 or 2 mg/kg; *n* = 11–12/group). Plasma methylmalonic acid concentrations were substantially decreased (>80% mean decrease compared to baseline) 1 week following the first IV dose of 0.5 or 2 mg/kg *hMUT* mRNA in MMA hypomorphic mice (Fig. 1a). A smaller reduction (31%) was observed in the

0.1 mg/kg *hMUT* mRNA group 1-day post-dose. A dose-dependent rebound to near-baseline concentrations was observed with the 0.1, 0.5, and 2.0 mg/kg *hMUT* mRNA dose groups at 1, 2, and 3 weeks post-dose, respectively. In contrast, no metabolic response in plasma methylmalonic acid was observed in either control group (PBS and *eGFP* mRNA). Similar plasma biomarker responses were observed for 2 additional primary disease-associated toxic metabolites, 2-methylcitrate and C3/C2 carnitine ratio (Fig. 1b–c). Based on these data, a dosing interval of every 2 weeks was chosen for the remainder of the study. All hypomorphic mice received 5 additional IV bolus injections of PBS, *eGFP* mRNA, or *hMUT* mRNA every 2 weeks for the next 8 weeks. Similar to the first 4 weeks of the study, a dose-dependent biomarker response to *hMUT* mRNA was observed over the remainder of the study in contrast to control groups (PBS and *eGFP* mRNA) (Fig. 1a–c). Collectively these plasma biomarker data demonstrate the dose-dependent bioactivity of *hMUT* mRNA throughout the entirety of the 12-week study in MMA hypomorphic mice.

Methylmalonic acid and 2-methylcitrate concentrations were assessed in key disease tissues (liver, kidney, and skeletal muscle) at the end of the 12-week study. Concentrations of both biomarkers were significantly lower (*p* < .05 from Tukey's pairwise comparison following a one-way ANOVA) in all key disease tissues in hypomorphic mice treated with 0.5 and 2 mg/kg *hMUT* mRNA compared to PBS and *eGFP* mRNA controls (Fig. 1d). Indeed, hypomorphic mice treated with 0.5 and 2 mg/kg *hMUT* mRNA had nearly undetectable levels of these biomarkers in liver, similar to unaffected *Mut*^{+/-} littermate mice.

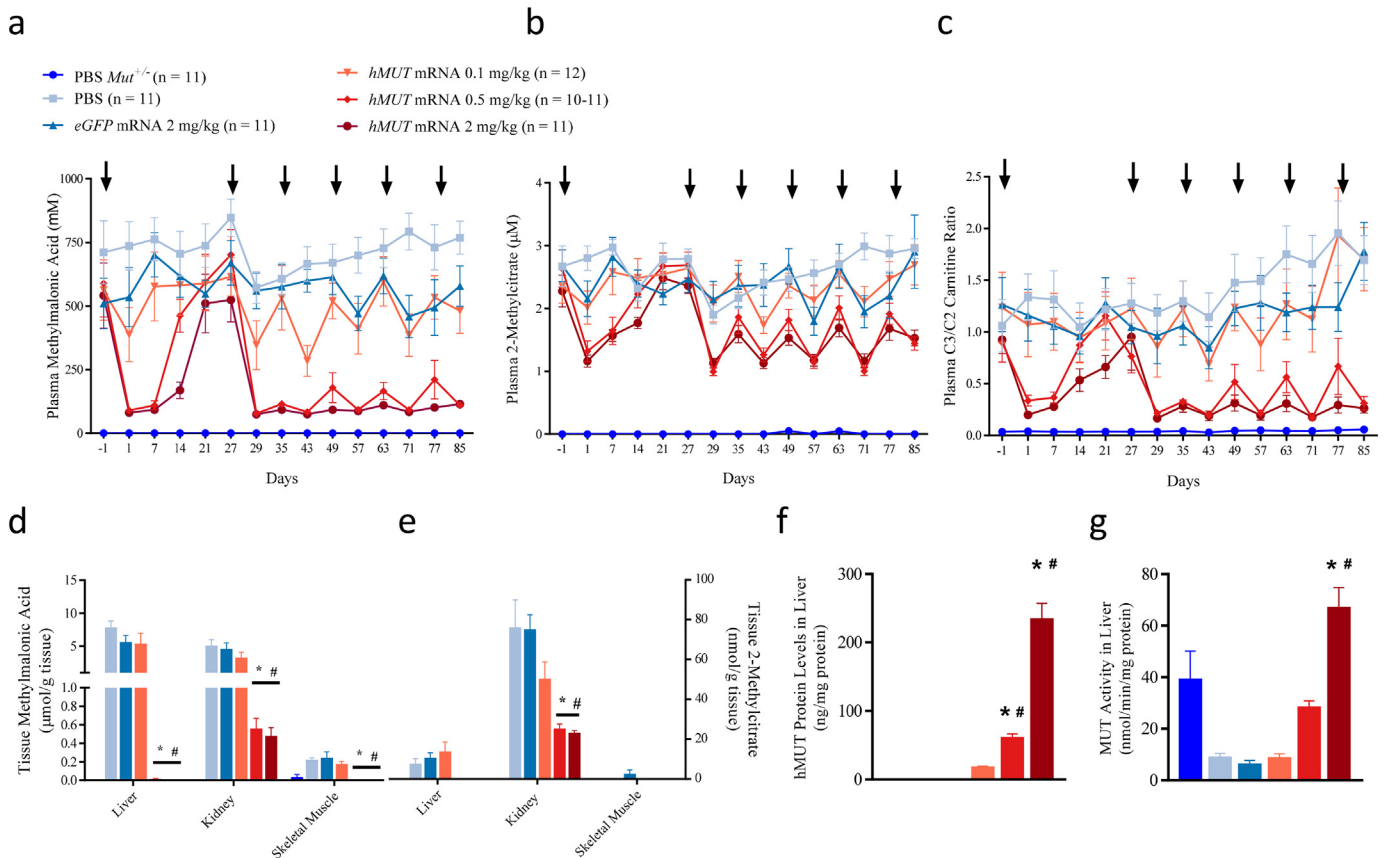


Fig. 1. *hMUT* mRNA treatment ameliorates disease biomarkers and restores functional MUT protein in liver in MMA hypomorphic mice. (a–c) *Mut*^{-/-};Tg^{INS-CBA-G715V} hypomorphic mice received repeat IV injections of either PBS control, *eGFP* mRNA control (2 mg/kg), or *hMUT* mRNA (0.1, 0.5 or 2 mg/kg) formulated in LNPs (*n* = 10–12/group) and were monitored for plasma methylmalonic acid (a), 2-methylcitrate (b) and C3/C2 carnitine ratio (c). An additional cohort of unaffected *Mut*^{+/-} mice received repeat IV injections of PBS. Arrows denote timing of IV administration of test and control articles (weeks 0, 4, 6, 8, 10, 12). (d–e) Methylmalonic acid (d) and 2-methylcitrate (e) concentrations were assessed in key disease tissues (liver, kidney, and skeletal muscle) at the end of the 12-week study (24 h after last dose, *n* = 10–12/group). (f–g) *hMUT* protein concentrations (f) and total MUT enzyme activity (g) were assessed in liver at the end of the 12-week study (24 h after the last dose, *n* = 10–12/group). Data presented as mean ± SEM. **p* < .05 compared to PBS-injected *Mut*^{-/-};Tg^{INS-CBA-G715V} group, #*p* < .05 compared to *eGFP* mRNA-injected *Mut*^{-/-};Tg^{INS-CBA-G715V} group from Tukey's pairwise comparison test following a one-way ANOVA (D–G).

3.2. Dose-dependent restoration of functional MUT enzyme in liver due to *hMUT* mRNA in MMA hypomorphic mice

hMUT mRNA treatment resulted in dose-dependent increases in hepatic *hMUT* protein and enzyme activity at the end of the 12-week study. Hepatic *hMUT* protein concentrations, quantified with an LC-MS/MS method using a human-specific detection peptide, were 18.1 ± 3.3 , 61.2 ± 15.3 and 234.6 ± 75.6 ng/mg protein in mice treated with 0.1, 0.5 and 2 mg/kg *hMUT* mRNA, respectively (Fig. 1f). Similarly, liver MUT enzyme activity levels were 8.8 ± 5.4 , 28.5 ± 7.4 and 67.1 ± 25.7 nmol/min/mg protein in mice treated with 0.1, 0.5 and 2 mg/kg *hMUT* mRNA, respectively (Fig. 1g).

To determine the bio-distribution of mRNA expressed *hMUT* protein, a separate single dose study was performed. *Mut*^{-/-};Tg^{INS-CBA-G715V} mice received a single IV bolus dose administration of LNP-encapsulated *hMUT* mRNA (n = 18) or *eGFP* mRNA (n = 12) at 0.5 mg/kg and were sacrificed at 24 h. *hMUT* protein concentrations in six tissues (liver, spleen, kidney, heart, lung and lymph node) were measured by LC-MS/MS. *hMUT* protein concentrations were 65.3 ± 40.8 and 0.6 ± 0.4 ng/mg protein in liver and spleen, respectively, and not detectable in the remaining tissues (kidney, heart, lung, lymph node) in mice administered *hMUT* mRNA (Fig. S3). *hMUT* protein was undetectable in all evaluated tissues in *eGFP* mRNA-injected mice.

3.3. *hMUT* mRNA therapy was well-tolerated in MMA hypomorphic mice

To evaluate the safety and tolerability of *hMUT* mRNA therapy in MMA hypomorphic mice, clinical observations and body weights were monitored throughout the 12-week study. Clinical observations were performed at least 5 times per week. No *hMUT* mRNA-related clinical findings were identified throughout the entirety of the study. Body weights and body weight gains were similar between all groups throughout the study, including unaffected *Mut*^{+/-} littermate mice (Fig. S1).

Clinical chemistry was additionally evaluated at the end of the study in all mice (Fig. 2 & Table S4). Across all clinical chemistry parameters, no toxicologically-relevant findings were observed. Importantly, no increase in markers of liver toxicity was observed in *hMUT* mRNA treated mice compared to PBS-injected hypomorphic mice (Fig. 2a–h and Table S4). When compared to phenotypically normal *Mut*^{+/-} mice, a slight yet statistically significant increase of liver enzymes (serum AST, ALT, ALP) was observed in PBS-injected MMA hypomorphic mice suggesting mild liver changes in affected mice (Fig. 2a–c). This is further supported by mild decreases in total protein, albumin, globulin and cholesterol in PBS-injected hypomorphic mice compared to unaffected *Mut*^{+/-} mice (Fig. 2d–f and i). In contrast, treatment with 0.5 and 2 mg/kg *hMUT* mRNA led to dose-dependent reductions in all liver enzymes and increases in total protein, albumin, globulin, and cholesterol, suggesting improved liver health in MMA hypomorphic mice due to mRNA therapy. Additionally, minimal decreases in serum albumin/globulin ratio, sodium, and chloride were observed in *hMUT* mRNA-treated versus PBS-injected hypomorphic mice (Fig. 2g and j–k).

3.4. Histopathology examination revealed minimal microscopic findings in spleen and potential improvement in hepatic pathology due to *hMUT* mRNA therapy

Histopathology examination of a full set of tissues (Table S5) was performed at the end of the 12-week study to further evaluate the safety of *hMUT* mRNA therapy. No gross pathological findings related to *hMUT* mRNA were observed in any tissues. Across all examined tissues, *hMUT* mRNA-related microscopic findings were limited to the spleen where a dose-dependent increase in minimal to mild lymphoid depletion of the periarteriolar lymphoid sheath was observed (Table 1). This finding was characterized by a decrease in lymphocytes in the region adjacent to the

central arteries (Fig. S2). In addition, a dose-dependent increase in red pulp cellularity in spleen was observed in MMA hypomorphic mice treated with *hMUT* mRNA (Fig. S2). These findings were likely related to the LNP as they were also observed with similar incidence in hypomorphic mice administered *eGFP* mRNA formulated in the same LNPs at 2 mg/kg.

In the liver, a minimal increase in mitotic figures and centrilobular hepatocellular hypertrophy was observed in 17.6% (6/34) of hypomorphic mice administered PBS, *eGFP* mRNA or *hMUT* mRNA at the low dose (0.1 mg/kg) (Table 1, Fig. 2l–n). These findings were not identified in unaffected *Mut*^{+/-} littermate mice administered PBS nor in hypomorphic mice receiving higher, efficacious dose levels of *hMUT* mRNA (0.5 mg/kg and 2 mg/kg) (Table 1, Fig. 2l–n). The absence of these degenerative findings in mice treated with efficacious dose levels of *hMUT* mRNA is suggestive of a beneficial effect of *hMUT* mRNA on liver pathology.

3.5. *hMUT* mRNA therapy improved survival, growth, and metabolic disturbances in a 12-week study in severe MMA mice

The efficacious dose level and regimen of *hMUT* mRNA was further evaluated in a separate 12-week pharmacology study in a severe mouse model of MMA, *Mut*^{-/-};Tg^{INS-MCK-Mut}. We have previously shown that there is no difference in survival between *Mut*^{-/-};Tg^{INS-MCK-Mut} mice that received control mRNA and untreated mice [19]. Additionally, the 12-week study in MMA hypomorphic mice showed no differences in disease biomarkers and metabolic characteristics between mice injected with *eGFP* mRNA vs. PBS. Therefore, we did not include a control mRNA group in the 12-week study in *Mut*^{-/-};Tg^{INS-MCK-Mut} mice. Repeat IV administration of *hMUT* mRNA at 0.5 mg/kg every 2 weeks resulted in a pronounced and highly significant improvement in survival in severe MMA mice (n = 6/group, $p < .001$ from log-rank test, Fig. 3a). All *hMUT* mRNA treated mice survived the entire duration of the 12-week study similar to PBS-injected unaffected *Mut*^{+/-} mice (Fig. 3a). In marked contrast, PBS-injected severe MMA mice exhibited a precipitous decline in survival (median study day of death: 1.5 days).

hMUT mRNA-treated mice thrived, as demonstrated by their substantial improvement in growth. Mean body weights of *hMUT* mRNA-treated mice increased 2.7-fold during the 12-week study (Fig. 3b). Indeed, the body weights of *hMUT* mRNA-treated mice approached the body weights of unaffected *Mut*^{+/-} littermate mice. In contrast, PBS-injected severe MMA mice gained minimal weight during the period that they survived.

Correlated with the improvement in survival and growth, *hMUT* mRNA-treated mice showed clear and consistent decreases in all 3 plasma biomarkers 1 day and 1 week after each dose administration (Fig. 3c–e). In contrast, these biomarkers showed no metabolic response and high variability in PBS-treated MMA mice (Fig. S4).

Tissue methylmalonic acid and 2-methylcitrate concentrations were evaluated in key disease tissues (liver, kidney, skeletal muscle, heart, brain) of surviving mice at the end of the 12-week study. All PBS-injected severe MMA mice perished by week 5 of the study (Fig. 3A) and thus were not available for tissue biomarker evaluation. To determine biomarker concentrations in untreated mice, tissue biomarkers were also evaluated in a slightly younger cohort of severe MMA mice (6–11 weeks old, n = 5). Tissue methylmalonic acid and 2-methylcitrate concentrations were 45–100% lower in *hMUT* mRNA versus PBS-injected severe MMA mice (Fig. 3f–g). Of note, liver biomarker levels were depleted to normal levels in *hMUT* mRNA-treated MMA mice.

hMUT mRNA treatment restored functional MUT enzyme in liver in severe MMA mice (Fig. 3h–i). Following 12 weeks of treatment, *hMUT* protein and activity were detected in liver at concentrations of 113 ± 44.7 ng/mg protein and 23.6 ± 10.3 nmol/min/mg protein 24 h after the last dose (Fig. 3h–i).

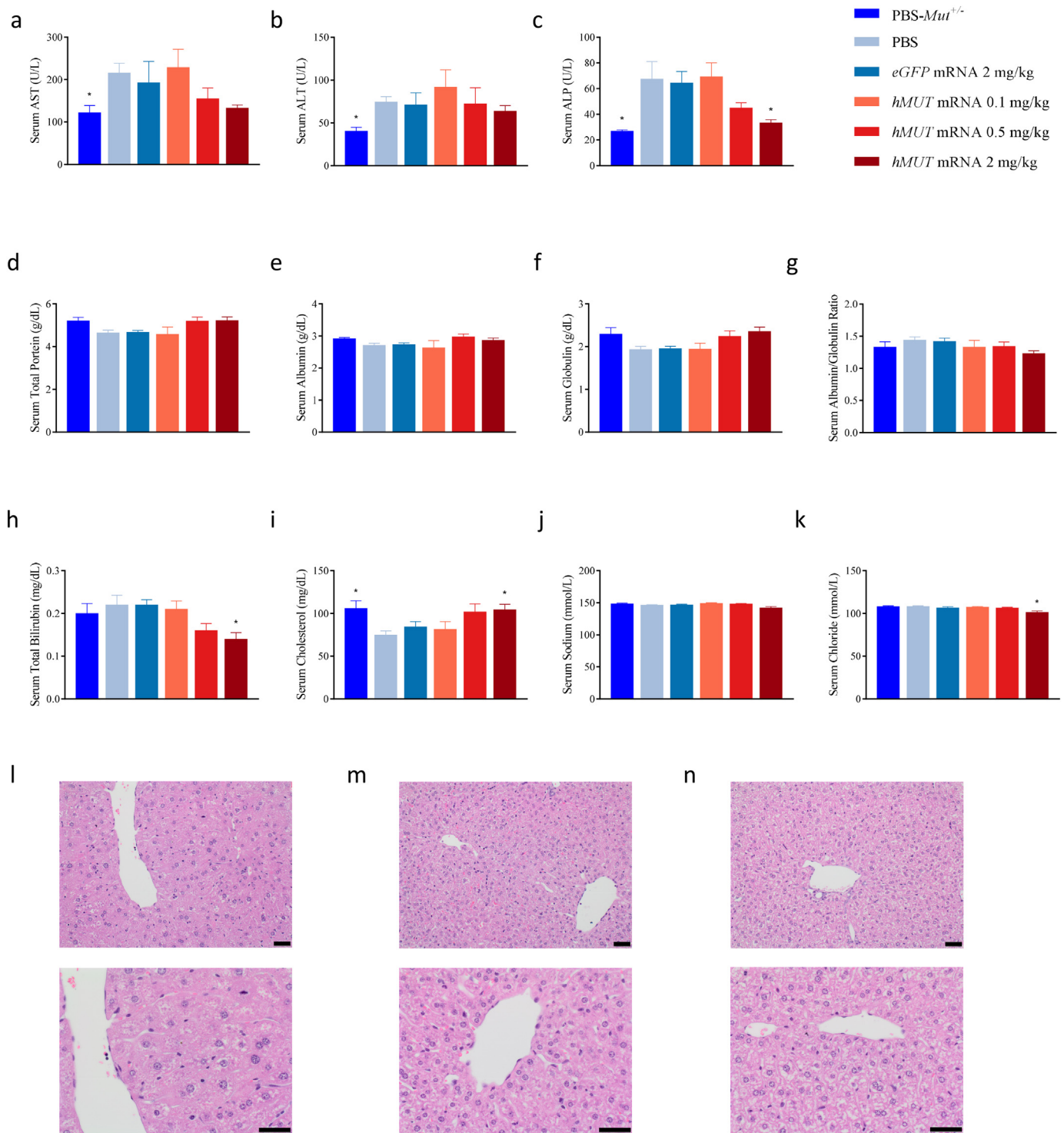


Fig. 2. Minimal changes in clinical chemistry parameters and improved liver histopathology in MMA hypomorphic mice after repeated *hMUT* mRNA treatment. (a–i) Select clinical chemistry (serum AST, ALT, ALP, total protein, globulin, albumin, albumin/globulin ratio, total bilirubin, and cholesterol) in *Mut*^{+/+} and PBS, *eGFP* mRNA and *hMUT* mRNA-treated hypomorphic mice ($n = 10\text{--}12/\text{group}$). (j–k) Select clinical chemistry electrolytes (serum sodium and chloride) in *Mut*^{+/+} and PBS, *eGFP* mRNA and *hMUT* mRNA-treated hypomorphic mice ($n = 6\text{--}9/\text{group}$). (l–n) Histology of the liver was examined and representative images of *Mut*^{-/-};Tg^{INS-CBA-G715V} mice injected with PBS (l) and *hMUT* mRNA 0.5 mg/kg (m) and *Mut*^{+/+} (n) are presented. Data presented as mean \pm SEM. * $p < .05$ compared to *Mut*^{-/-};Tg^{INS-CBA-G715V} PBS group obtained from Dunn's multiple comparisons test following a Kruskal-Wallis test.

Finally, in this study, mice were monitored for clinical observations throughout the study at least 5 times per week. No clinical signs were observed in *hMUT* mRNA-treated mice. The lack of clinical observations combined with the survival and body weight data suggest that *hMUT* mRNA was well-tolerated in severe MMA mice.

4. Discussion

Despite dietary and supportive management, MMA patients, particularly *mut*⁰ patients, suffer high morbidity and mortality. Conventional enzyme replacement therapy is currently not a viable treatment modality for MMA and many other inborn errors of metabolism due to

Table 1
Summary of microscopic findings in spleen and liver in 12-week study in MMA hypomorphic mice.

Genotype		<i>Mut</i> ^{+/-}		<i>Mut</i> ^{-/-} ;Tg ^{INS-CBA-G715V}				
		PBS		eGFP mRNA	hMUT mRNA			
Treatment		PBS		eGFP mRNA	hMUT mRNA			
Dose (mg/kg)		NA		2	0.1	0.5	2	
n		11		11	11	12	10	11
Spleen								
Lymphoid depletion PALS ^a	Minimal	0 (0%)		7 (63.6%)	1 (8.3%)	9 (90.0%)	9 (81.8%)	
	Mild	0 (0%)		0 (0%)	0 (0%)	0 (0%)	1 (9.1%)	
Increased cellularity (red pulp)	Minimal	0 (0%)		8 (72.7%)	0 (0%)	8 (80.0%)	10 (90.9%)	
Liver								
Hepatocellular hypertrophy	Minimal	0 (0%)		3 (27.3%)	1 (9.1%)	1 (8.3%)	0 (0%)	
Increased mitosis	Minimal	0 (0%)		3 (27.3%)	0 (0%)	3 (25.0%)	0 (0%)	

^a PALS = peri-arteriolar lymphoid sheaths. Data presented as n (%).

technical challenges in producing complex recombinant enzymes that require specialized subcellular localizations. Exogenous mRNA, in principle, can produce any type of complex protein by using the cell's endogenous translational machinery. In previous proof-of-concept studies, we demonstrated that LNP-encapsulated *hMUT* mRNA encoded functional MUT enzyme in liver, reduced disease-associated metabolites, and ultimately improved survival upon repeat dosing in a 6-week study. However, comprehensive long-term efficacy, safety and tolerability studies in relevant animal models are required to support the clinical development of *hMUT* mRNA therapy for this pediatric population.

Here, we demonstrate sustained bioactivity and pharmacology of *hMUT* mRNA in two long-term repeat dose studies in two murine models of MMA. Reproducible and marked decreases in plasma methylmalonic acid, 2-methylcitrate and C3/C2 carnitine ratio were observed following each dose administration of LNP-encapsulated *hMUT* mRNA in both murine models. These biomarker reductions correlated with remarkable improvements in survival and growth in severe MMA mice over the span of 12 weeks. The magnitude of plasma methylmalonic acid reductions was similar to decreases observed following LT in MMA patients [10,11]. Although all plasma biomarkers were substantially decreased, they were not reduced to normal levels. Complete normalization of plasma methylmalonic acid and other biomarkers was not expected, similar to transplanted patients [10,11], due to production of toxins in other high energy organs such as skeletal muscle, heart and brain.

The liver, and more specifically the hepatocyte, is regarded as the major target for mitochondrial pathology in MMA [29]. *hMUT* mRNA restored functional MUT enzyme in liver and as a direct consequence, depleted toxic metabolite concentrations in livers of MMA mice. Liver from patients and murine models of MMA have a mega-mitochondrial phenotype that is readily visible using electron microscopy [29,37]. Although electron microscopy was not performed in the current study, light microscopy analysis of liver tissues revealed an increase in hepatocellular hypertrophy in control hypomorphic mice that may be due to enlarged mitochondria. Interestingly, hepatocellular hypertrophy was not observed in hypomorphic mice treated with efficacious dose levels of *hMUT* mRNA or in unaffected littermate control mice. Additionally, mild liver chemistry abnormalities were observed in untreated MMA hypomorphic mice compared to unaffected mice. This is consistent with published reports from the European registry and network for intoxication type metabolic diseases, in which a small fraction (<20%) of MMA patients had abnormal liver function tests [38]. Other laboratory and ultrasound measured liver abnormalities have been described in MMA patients [39]. *hMUT* mRNA treatment normalized most of the altered liver function parameters in a dose-dependent manner in hypomorphic mice, suggesting a potential improvement on liver health. These data, combined with the depletion of hepatic toxic metabolites and improved liver function tests, suggest an overall improvement in liver pathology due to *hMUT* mRNA.

Impaired mitochondrial function observed in key extrahepatic disease tissues (kidney, heart, skeletal muscle, and brain) from MMA patients may contribute to long-term complications associated with this disease [29,40–48]. The molecular mechanisms of mitochondrial dysfunction in these key disease tissues are not fully understood but are hypothesized to be partially caused by accumulation of toxic metabolites such as methylmalonic acid and 2-methylcitrate [49]. Although *hMUT* mRNA is a liver-focused therapy, significant decreases in tissue methylmalonic acid and 2-methylcitrate concentrations were seen in extrahepatic tissues. As there was no detectable increase in MUT enzyme produced in these extrahepatic tissues, these tissue biomarker reductions were likely due to decreases in circulating toxic metabolites. Recent single-center reports describe renal and neurological stabilization or improvement following LT in patients with MMA [10,11], however, other studies have reported renal and neurologic deterioration post-LT [9,50]. The long-term outcomes, particularly renal and neurologic progression, following LT remain to be fully described. Whether a liver-focused therapy such as *hMUT* mRNA has a beneficial effect on extrahepatic clinical manifestations will have to be determined in clinical trials. Early intervention in the disorder may, in theory, prevent irreversible insults to various extrahepatic organs during metabolic decompensations, although further research is warranted.

The safety and tolerability of repeat IV administration of *hMUT* mRNA encapsulated in LNPs were evaluated in hypomorphic mice. *hMUT* mRNA was well-tolerated, as demonstrated by the lack of any *hMUT* mRNA-related clinical findings and similar body weights across treatment and control groups. Clinical chemistry and histopathology findings were limited and are likely due to a non-specific, generalized inflammatory state that is likely transient and not considered to be adverse. Due to blood volume limitations, hematology, cytokines, and complement factors were not evaluated in the current study. Nevertheless, we have previously evaluated inflammatory markers in a 5-week repeat dose study in MMA hypomorphic mice [19]. No increase of plasma cytokines (IL-6, IFN- γ , TNF- α , IL-1 β) was observed in MMA hypomorphic mice following 3 and 5 weekly IV bolus injections of *hMUT* mRNA (0.2 mg/kg) compared to mice receiving weekly injections of PBS. Moreover, minimal elevations in inflammatory markers including complement and cytokines have been observed in repeat dose toxicology studies conducted in cynomolgus monkeys receiving mRNA encapsulated with a similar LNP (1 mg/kg) [23]. Furthermore, even if inflammatory markers were aberrant, the histopathology examination across a full panel of tissues did not identify any obvious microscopic correlate. Although anti-drug antibodies were not evaluated in the current studies, the consistent and reproducible pharmacologic response following each mRNA dose suggests that no neutralizing antibodies were developed. Furthermore, preclinical evaluation of immunogenicity has limited translation to humans and thus, anti-drug antibodies should be carefully monitored in clinical trials. Common strategies used to mitigate deleterious anti-drug antibodies such as immunomodulatory and/or premedication regimens could be considered as clinical data emerge.

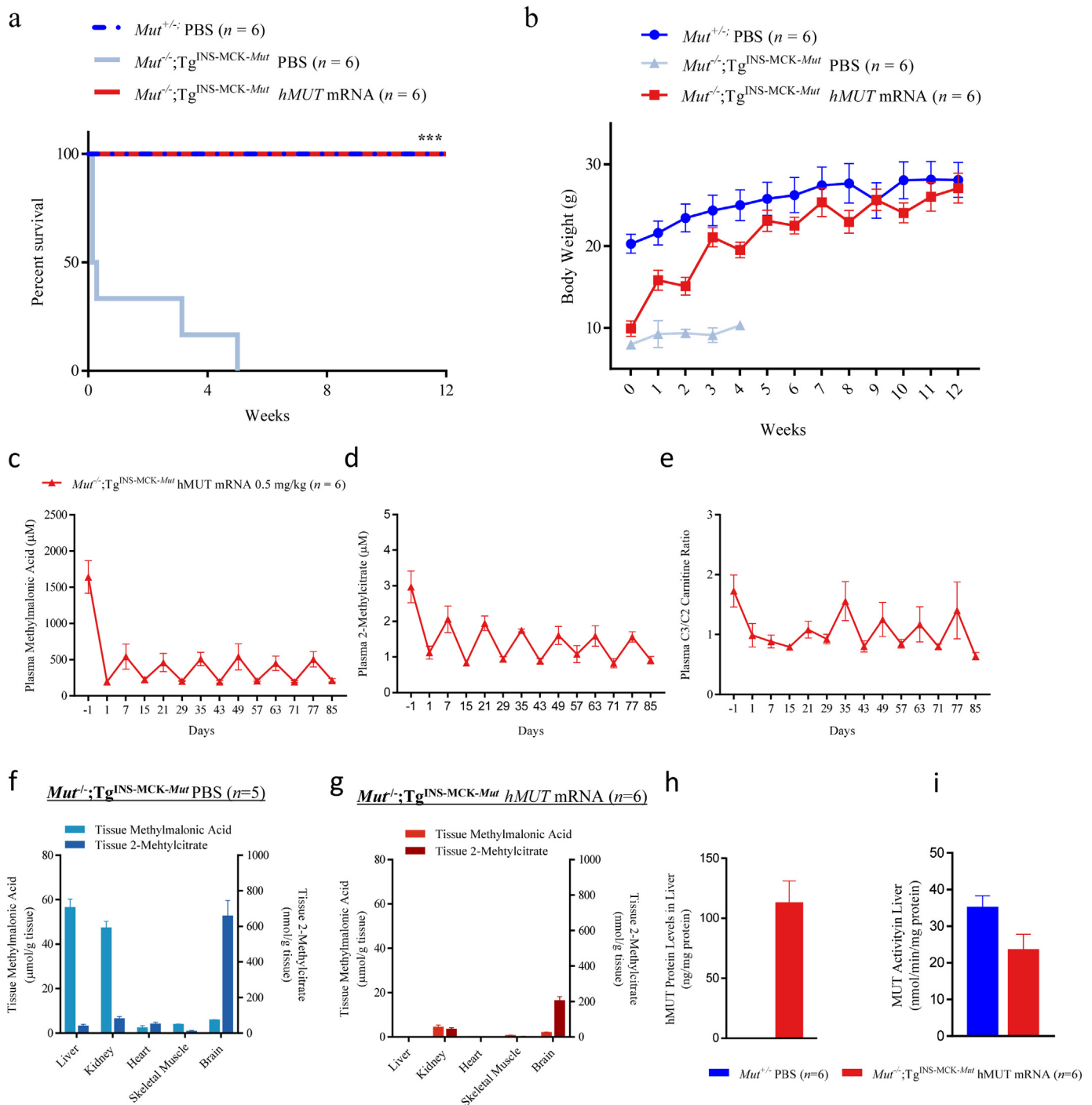


Fig. 3. *hMUT* mRNA improves survival and growth, reduces disease biomarkers and restores functional MUT enzyme in severe MMA $Mut^{-/-};Tg^{INS-MCK-Mut}$ mice. (a) Kaplan-Meier survival curves of severe MMA $Mut^{-/-};Tg^{INS-MCK-Mut}$ mice receiving every other week IV bolus injections of *hMUT* mRNA 0.5 mg/kg or PBS ($n = 6$ /group). *** $p < .001$ from log-rank test. Survival curve of unaffected $Mut^{+/-}$ mice receiving IV injections of PBS ($n = 6$) additionally shown. (b) Body weight was monitored weekly throughout the 12-week study. $n = 6$ for *hMUT* mRNA-treated $Mut^{-/-};Tg^{INS-MCK-Mut}$ and PBS-injected $Mut^{+/-}$ mouse groups. $n = 6, 2, 2, 2, 2, 1$ at study weeks 1, 2, 3, 4, and 5 respectively for PBS-injected $Mut^{-/-};Tg^{INS-MCK-Mut}$ group. (c–e) Plasma methylmalonic acid (c), 2-methylcitrate (d), and C3/C2 carnitine ratio (e) were serially monitored weekly throughout the 12-week study. (f–g) Methylmalonic acid and 2-methylcitrate concentrations were assessed in key disease tissues (liver, kidney, heart, brain and skeletal muscle) 24 h after a single injection of PBS (f) and at the end of 12-weeks of treatment of *hMUT* mRNA (g) in $Mut^{-/-};Tg^{INS-MCK-Mut}$ mice ($n = 5–6$ /group). (h–i) *hMUT* protein concentrations (h) and total MUT enzyme activity (i) were assessed in liver at the end of the 12-week study (24 h after the last dose administration) in *hMUT* mRNA-treated $Mut^{-/-};Tg^{INS-MCK-Mut}$ mice and PBS-injected unaffected $Mut^{+/-}$ mice ($n = 6$ /group). Data presented as mean \pm SEM.

As systemic *hMUT* mRNA therapy will require chronic, repeat IV infusions every few weeks, the clinical adoption of such a therapy remains to be determined in this disorder. However, this dosing regimen is similar to several enzyme replacement therapies prescribed for multiple lysosomal storage disorders (e.g. Fabry, Gaucher, and Mucopolysaccharidoses). Additionally, clinical implementation of a

potential mRNA therapy will largely be influenced by safety and efficacy results from upcoming clinical trials in patients and ultimately, the cost-effectiveness of the therapy.

In summary, results from two long-term studies demonstrate sustained pharmacology and durable functional benefit for *hMUT* mRNA in two murine models of MMA representing the spectrum of

MUT deficiency. *hMUT* mRNA therapy was well-tolerated with no adverse side effects in both mouse models. These data collectively support the clinical development of *hMUT* mRNA therapy in this devastating pediatric disorder with no effective treatment options other than elective solid organ transplantation.

Acknowledgements

The authors thank Dr. Charles Venditti at NHGRI/NIH for licensing the two murine models of MMA. The authors thank Katherine Kacena for performing statistical analyses.

Funding source

This work was funded by Moderna, Inc. Funders had no role in study design, data collection, data analysis, interpretation or writing of the report.

Declaration of interests

All authors are employees of, and receive salary and stock options from Moderna, Inc.

Author contributions

D.A., A.F., and L.T.G. designed the experiments. D.A., A.F., E.J., M.E., C.D., V.N. and J. Milton performed the experiments. D.A., A.F., E.J., J.M., R.L. and L.T.G. analyzed the data. L.T.G. and D.A. wrote the manuscript, and all authors edited the manuscript.

Appendix A. Supplementary data

Supplementary data to this article can be found online at <https://doi.org/10.1016/j.ebiom.2019.07.003>.

References

- Manoli I, Sloan JL, Venditti CP. Isolated Methylmalonic Acidemia. In: Pagon RA, Adam MP, Ardinger HH, Wallace SE, Amemiya A, Bean LJH, et al, editors. GeneReviews(R); 1993 Seattle (WA).
- Forny P, Schnellmann AS, Buerer C, Lutz S, Fowler B, Froese DS, et al. Molecular genetic characterization of 151 Mut-type Methylmalonic aciduria patients and identification of 41 novel mutations in MUT. *Hum Mutat* 2016;37(8):745–54.
- Zwickler T, Haeghe G, Riderer A, Horster F, Hoffmann GF, Burgard P, et al. Metabolic decompensation in methylmalonic aciduria: which biochemical parameters are discriminative? *J Inher Metab Dis* 2012;35(5):797–806.
- Fraser JL, Venditti CP. Methylmalonic and propionic acidemias: clinical management update. *Curr Opin Pediatr* 2016;28(6):682–93.
- Baumgartner MR, Horster F, Dionisi-Vici C, Haliloglu G, Karall D, Chapman KA, et al. Proposed guidelines for the diagnosis and management of methylmalonic and propionic acidemia. *Orphanet J Rare Dis* 2014;9:130.
- Horster F, Baumgartner MR, Viardot C, Suormala T, Burgard P, Fowler B, et al. Long-term outcome in methylmalonic acidurias is influenced by the underlying defect (mut0, Mut-, cblA, cblB). *Pediatr Res* 2007;62(2):225–30.
- Hussein MH, Hashimoto T, Suzuki T, Daoud GA, Goto T, Nakajima Y, et al. Children undergoing liver transplantation for treatment of inherited metabolic diseases are prone to higher oxidative stress, complement activity and transforming growth factor-beta1. *Ann Transplant* 2013;18:63–8.
- Kamei K, Ito S, Shigeta T, Sakamoto S, Fukuda A, Horikawa R, et al. Preoperative dialysis for liver transplantation in methylmalonic acidemia. *Ther Apher Dial* 2011;15(5):488–92.
- Kasahara M, Horikawa R, Tagawa M, Uemoto S, Yokoyama S, Shibata Y, et al. Current role of liver transplantation for methylmalonic acidemia: a review of the literature. *Pediatr Transplant* 2006;10(8):943–7.
- Niemi AK, Kim IK, Krueger CE, Cowan TM, Baugh N, Farrell R, et al. Treatment of methylmalonic acidemia by liver or combined liver-kidney transplantation. *J Pediatr* 2015;166(6):1455–1461 e1.
- Crittelli K, McKiernan P, Vockley J, Mazariegos G, Squires RH, Soltys K, et al. Liver transplantation for propionic Acidemia and Methylmalonic Acidemia: perioperative management and clinical outcomes. *Liver Transpl* 2018;24(9):1260–70.
- Chen PW, Hwu WL, Ho MC, Lee NC, Chien YH, Ni YH, et al. Stabilization of blood methylmalonic acid level in methylmalonic acidemia after liver transplantation. *Pediatr Transplant* 2010;14(3):337–41.
- Pardi N, Tuyishime S, Muramatsu H, Kariko K, Mui BL, Tam YK, et al. Expression kinetics of nucleoside-modified mRNA delivered in lipid nanoparticles to mice by various routes. *J Control Release* 2015;217:345–51.
- Pardi N, Secreto AJ, Shan X, Debonera F, Glover J, Yi Y, et al. Administration of nucleoside-modified mRNA encoding broadly neutralizing antibody protects humanized mice from HIV-1 challenge. *Nat Commun* 2017;8:14630.
- Kauffman KJ, Mir FF, Jhunjhunwala S, Kaczmarek JC, Hurtado JE, Yang JH, et al. Efficacy and immunogenicity of unmodified and pseudouridine-modified mRNA delivered systemically with lipid nanoparticles in vivo. *Biomaterials* 2016;109:78–87.
- Kauffman KJ, Dorkin JR, Yang JH, Heartlein MW, DeRosa F, Mir FF, et al. Optimization of lipid nanoparticle formulations for mRNA delivery in vivo with fractional factorial and definitive screening designs. *Nano Lett* 2015;15(11):7300–6.
- Ramaswamy S, Tonnun N, Tachikawa K, Limphong P, Vega JB, Karmali PP, et al. Systemic delivery of factor IX messenger RNA for protein replacement therapy. *Proc Natl Acad Sci U S A* 2017;114(10):E1941–50.
- Cullis PR, Hope MJ. Lipid nanoparticle systems for Enabling Gene Therapies. *Mol Ther* 2017;25(7):1467–75.
- An D, Schneller JL, Frassetto A, Liang S, Zhu X, Park JS, et al. Systemic messenger RNA therapy as a treatment for Methylmalonic Acidemia. *Cell Rep* 2017;21(12):3548–58.
- Jiang L, Berraondo P, Jerico D, Guey LT, Sampedro A, Frassetto A, et al. Systemic messenger RNA as an etiological treatment for acute intermittent porphyria. *Nat Med* 2018;24(12):1899–909.
- Prieve MG, Harvie P, Monahan SD, Roy D, Li AG, Blevins TL, et al. Targeted mRNA therapy for ornithine Transcarbamylase deficiency. *Mol Ther* 2018;26(3):801–13.
- Roseman DS, Khan T, Rajas F, Jun LS, Asrani KH, Isaacs C, et al. G6PC mRNA therapy positively regulates fasting blood glucose and decreases liver abnormalities in a mouse model of glycogen storage disease 1a. *Mol Ther* 2018;26(3):814–21.
- Sabnis S, Kumarasinghe ES, Salerno T, Mihai C, Ketova T, Senn JJ, et al. A novel amino lipid series for mRNA delivery: improved endosomal escape and sustained pharmacology and safety in non-human primates. *Mol Ther* 2018;26(6):1509–19.
- DeRosa F, Guild B, Karve S, Smith L, Love K, Dorkin JR, et al. Therapeutic efficacy in a hemophilia B model using a biosynthetic mRNA liver depot system. *Gene Ther* 2016;23(10):699–707.
- Zhu X, Yin L, Theisen M, Zhuo J, Siddiqui S, Levy B, et al. Systemic mRNA therapy for the treatment of Fabry disease: preclinical studies in wild-type mice, Fabry mouse model, and wild-type non-human primates. *Am J Hum Genet* 2019;104(4):625–37.
- Richner JM, Himansu S, Dowd KA, Butler SL, Salazar V, Fox JM, et al. Modified mRNA vaccines protect against Zika virus infection. *Cell* 2017;168(6):1114–1125 e10.
- Akinc A, Zumbuhl A, Goldberg M, Leshchiner ES, Busini V, Hossain N, et al. A combinatorial library of lipid-like materials for delivery of RNAi therapeutics. *Nat Biotechnol* 2008;26(5):561–9.
- Leung AK, Tam YY, Chen S, Hafez IM, Cullis PR. Microfluidic mixing: a general method for encapsulating macromolecules in lipid nanoparticle systems. *J Phys Chem B* 2015;119(28):8698–706.
- Chandler RJ, Zerfas PM, Shanske S, Sloan J, Hoffmann V, DiMauro S, et al. Mitochondrial dysfunction in Mut methylmalonic acidemia. *FASEB J* 2009;23(4):1252–61.
- Chandler RJ, Tsai MS, Dorko K, Sloan J, Korson M, Freeman R, et al. Adenoviral-mediated correction of methylmalonyl-CoA mutase deficiency in murine fibroblasts and human hepatocytes. *BMC Med Genet* 2007;8:24.
- Manoli I, Sysol J, Li L, Chandler R, Senac J, Hoffmann V, et al. Muscle targeted transgene expression rescues the lethal phenotype of Mut knockout mice. *Mol Genet Metab* 2011;102(3):248.
- Senac JS, Aswani VH, Sysol JR, Manoli I. C.P. V. Partial deficiency model of MUT Methylmalonic Acidemia (MMA) displays diet inducible disease and sensitivity to acetaminophen (APAP). *Mol Ther* 2013;21(1):S107.
- Chandler RJ, Sloan J, Fu H, Tsai M, Stabler S, Allen R, et al. Metabolic phenotype of methylmalonic acidemia in mice and humans: the role of skeletal muscle. *BMC Med Genet* 2007;8:64.
- Turgeon CT, Magera MJ, Cuthbert CD, Loken PR, Gavrilov DK, Tortorelli S, et al. Determination of total homocysteine, methylmalonic acid, and 2-methylcitric acid in dried blood spots by tandem mass spectrometry. *Clin Chem* 2010;56(11):1686–95.
- Minkler PE, Stoll MS, Ingalls ST, Yang S, Kerner J, Hoppel CL. Quantification of carnitine and acylcarnitines in biological matrices by HPLC electrospray ionization-mass spectrometry. *Clin Chem* 2008;54(9):1451–62.
- Quattara B, Duplessis M, Girard CL. Optimization and validation of a reversed-phase high performance liquid chromatography method for the measurement of bovine liver methylmalonyl-coenzyme a mutase activity. *BMC Biochem* 2013;14:25.
- Zsengeller ZK, Aljinovic N, Teot LA, Korson M, Rodig N, Sloan JL, et al. Methylmalonic acidemia: a megamitochondrial disorder affecting the kidney. *Pediatr Nephrol* 2014;29(1):2139–46.
- Kolker S, Valayannopoulos V, Burlina AB, Sykut-Cegielska J, Wijburg FA, Teles EL, et al. The phenotypic spectrum of organic acidurias and urea cycle disorders. Part 2: the evolving clinical phenotype. *J Inher Metab Dis* 2015;38(6):1059–74.
- Imbard A, Garcia Segarra N, Tardieu M, Broue P, Bouchereau J, Pichard S, et al. Long-term liver disease in methylmalonic and propionic acidemias. *Mol Genet Metab* 2018;123(4):433–40.
- de Keyzer Y, Valayannopoulos V, Benoist JF, Batteux F, Lacaille F, Hubert L, et al. Multiple OXPHOS deficiency in the liver, kidney, heart, and skeletal muscle of patients with methylmalonic aciduria and propionic aciduria. *Pediatr Res* 2009;66(1):91–5.
- Schuck PF, Rosa RB, Pettenuzzo LF, Sitta A, Wannmacher CM, Wyse AT, et al. Inhibition of mitochondrial creatine kinase activity from rat cerebral cortex by methylmalonic acid. *Neurochem Int* 2004;45(5):661–7.
- Ribeiro LR, Della-Pace ID, de Oliveira Ferreira AP, Funck VR, Pinton S, Bobinski F, et al. Chronic administration of methylmalonate on young rats alters neuroinflammatory markers and spatial memory. *Immunobiology* 2013;218(9):1175–83.

- [43] Pettenuzzo LF, Ferreira Gda C, Schmidt AL, Dutra-Filho CS, Wyse AT, Wajner M. Differential inhibitory effects of methylmalonic acid on respiratory chain complex activities in rat tissues. *Int J Dev Neurosci* 2006;24(1):45–52.
- [44] Jafari P, Braissant O, Zavadakova P, Henry H, Bonafe L, Ballhausen D. Brain damage in methylmalonic aciduria: 2-methylcitrate induces cerebral ammonium accumulation and apoptosis in 3D organotypic brain cell cultures. *Orphanet J Rare Dis* 2013;8:4.
- [45] Amaral AU, Cecatto C, Castilho RF, Wajner M. 2-Methylcitric acid impairs glutamate metabolism and induces permeability transition in brain mitochondria. *J Neurochem* 2016;137(1):62–75.
- [46] Wajner M, Goodman SI. Disruption of mitochondrial homeostasis in organic acidurias: insights from human and animal studies. *J Bioenerg Biomembr* 2011;43(1):31–8.
- [47] Ostergaard E, Wibrand F, Orngreen MC, Vissing J, Horn N. Impaired energy metabolism and abnormal muscle histology in Mut- methylmalonic aciduria. *Neurology* 2005;65(6):931–3.
- [48] Wilnai Y, Enns GM, Niemi AK, Higgins J, Vogel H. Abnormal hepatocellular mitochondria in methylmalonic acidemia. *Ultrastruct Pathol* 2014;38(5):309–14.
- [49] Morath MA, Okun JG, Muller IB, Sauer SW, Horster F, Hoffmann GF, et al. Neurodegeneration and chronic renal failure in methylmalonic aciduria—a pathophysiological approach. *J Inherit Metab Dis* 2008;31(1):35–43.
- [50] Kaplan P, Ficioglu C, Mazur AT, Palmieri MJ, Berry GT. Liver transplantation is not curative for methylmalonic acidopathy caused by methylmalonyl-CoA mutase deficiency. *Mol Genet Metab* 2006;88(4):322–6.